Reporting Class IV type AVO anomaly in deep waters of Indian basin

N.K. Khatri, N.C. Mandal, C. Mukhopadhyay, S. Hazra, A. Barua, A.K. Dwivedi and R.K. Sharma

Abstract

Class IV sands have been recorded in many basins throughout the world, including the Gulf of Mexico. Class IV type of AVO anomaly, possibly, has not been reported in Indian basins so far. Plio-Miocene gas sands are known to generate Class II to Class III type of AVO. Class IV occurs when the shear velocity of the overlain layer is higher than of the gas sand; which is the case when a porous gas sand is overlain by a high-velocity unit, such as a hard shale either siliceous or calcareous, siltstone, tightly cemented sand or a carbonate.While studying elastic curve derived from DSI and density well logs in Mahanadi basin, authors noticed the sand of anomalous elastic behavior having lesser Vs than overlaying shale, known to generate Class IV type of AVO anomaly. This has been discussed in this article.

Introduction

Intercept and gradient have their definition in Aki Richard approximation of Zoeppritz equation.

$$R(\theta) = A + B \sin^2\theta + C \tan^2\theta \sin^2\theta \quad \text{..... 1}$$

Equation for incident angle upto $\theta = 30$ 2

$$R(\theta) = A + B \sin^2\theta$$

Equation (2) Shows that $R(\theta)$ and $\sin^2\theta$ are linearly related; A and B as intercept and gradient respectively.

Where,

$$A = \frac{1}{2}\left[\frac{\Delta V_p}{V_p} + \frac{\Delta\rho}{\rho}\right]$$

$$B = \frac{1}{2}\frac{\Delta V_p}{V_p} - 4\left[\frac{V_s}{V_p}\right]\frac{\Delta V_s}{V_s} - 2\left[\frac{V_s}{V_p}\right]^2\frac{\Delta\rho}{\rho}$$

$$C = \frac{1}{2}\frac{\Delta V_p}{V_p}$$

where ΔV_p is the change in compressional velocity across the interface (Vp_2-Vp_1), V_P is the average compressional velocity across the interface (Vp_2 +Vp_1)/2, $\Delta\rho$ is the change indensity across the interface (ρ_1-ρ_2) and $\Delta\rho$ is the average density across the interface (P_1+P_2)/2, ΔVs is the change in shear velocity across the interface (Vs_2 -Vs_1), and ΔVs is the average shear velocity across the interface (Vs_2+Vs_1)/2, withVp1; Vs1; ρ1 and Vp2; Vs2; ρ2 being the medium properties in the first (overlying) and second (underlying) media, respectively.

Class I sands are high impedance relative to the overlying shale. In particular, for high-impedance gas sands, reflection coefficients decrease with increasing offset. Class II sands have impedance close to the overlying shale, therefore, low normal incidence reflectivity. Class III sands are lower impedance than the over lying shale, and exhibit increasing reflection magnitude with offset. In all these three classes the gas-sand reflection coefficients always become more negative with increasing offset i.e. B to be-ve. Class IV are lower impedance than the overlying shale, for which the reflection coefficient to become more positive with increasing offset i.e. B to be +ve, yet decrease in magnitude with increasing offset (Fig.1). Castagna et al introduced the Class IV type of AVO anomaly.

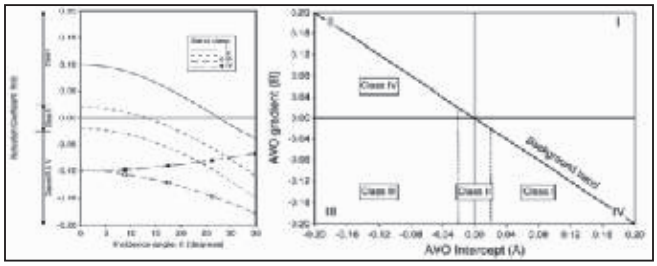

Fig. 1: Reflection coefficient and its variation with angle of incidence generating four type of AVO responses (Castagna, J.P. and Swan H.W., and Foster, D.J., 1998)

Richards and Frasier (1976) decomposition of equation (1) pertains to contribution to the reflection coefficient variation with offset from changes in Vp, Vs and ρ across the interface (Equation 3). It shows that Class IV anomaly appears, when change in Vs across the interface is negative which otherwise is positive in Class III type of AVO anomaly. (Castagna, J.P. and Swan H.W., 1997, Castagna, J.P. and Swan H.W., and Foster, D.J., 1998)

$$R(\theta) = \tfrac{1}{2}(1\text{-}4\,(Vs/Vp)2\sin^2\theta)\,\Delta\rho/(\rho)) + \tfrac{1}{2}(\cos^2\theta\,\Delta Vp/(Vp)) - 4\,(Vs/Vp)2\sin^2\theta\,\Delta Vs/(Vs); \quad (3)$$

Equation (3) shows contribution of -ve ΔVp, -ve $\Delta\rho$ and -ve ΔVs at θ=0 towards $R(\theta)$ is -Ve, -Ve and Zero respectively. It further shows contribution of amplitude variation with angles from negative ΔVp is to increase (more negative), from negative $\Delta\rho$ to decrease (more positive) and from positive ΔVs to increase amplitudes (more negative) resulting in total AVO response of class III i. e. the increase in amplitude with offset (more negative). Negative ΔVs gas sand top interface contributes to increase in amplitudes (more positive) with offset resulting total AVO response in decrease (more positive) in amplitude with offset i.e. is of class IV type. The

change from negative to positive gradient i.e class III to IV is due to thereversal of contribution from shear velocity component in two cases. (Castagna, J.P. and Swan H.W., 1997, Castagna, J.P. and Swan H.W., and Foster, D.J., 1998)

Class IV gas sands have a large negative A but positive B, therefore fall in quadrant II on A-B crossplots. Frasier decomposition for Low-impedance brine sands (therefore, lower shear impedance than shale) shows decrease in amplitude with offset like class IV gas sand case, which also falls in quadrant II as the background trend.

It is important to note that class IV gas sands are difficult to interpret on partial offset stacks or using product (A and B) indicators. However, they do get expressed on A-B cross plot and indicators such as Smith and Gidlow's fluid factor (Gidlow, P. M., Smith, G. C., and Vail, P. J., 1992).

Case: Porous Gas Charged and Brine Sands Overlain by Compact Shale

Three well Viz. A, B and C located in two of deep water blocks separated at distance of over 100Kms (Fig.2) are studied with the objective of understanding partial success of seismic AVO in Mahanadi basin. One meter of low acoustic impedance sand interval 3599.5 to 3600.5 in well B (water depths of ~1700mts) characterized by low GR, enough NPHI-RHOB cross over, but low resistivity and anomalous on elastic logs has shown 0.44% of gas while drilling in comparison to background gas of 0.1 to 0.17%. Resistivity does not support interval to be gas charged, but based on elastically anomalous behavior the interval has been interpreted to be marginally saturated gas sand (Fig.3). Encompassing shale, characterized by high gamma and well separated NPHI-RHOB have seen to be of higher resistivity, high density and high velocity is interpreted to be compacted. Marginally gas charged sand is moderately porous and have lesser Vs than encompassing shale besides lower impedance; an arrangement known to generate class IV type of anomaly.

Well logged Vp, Vs and density against marginally charged gas sand have been utilized to calculate Vp, Vs and density for brine sand using Gassmann equation/Castagna transform and density porosity relationand are given in table1.

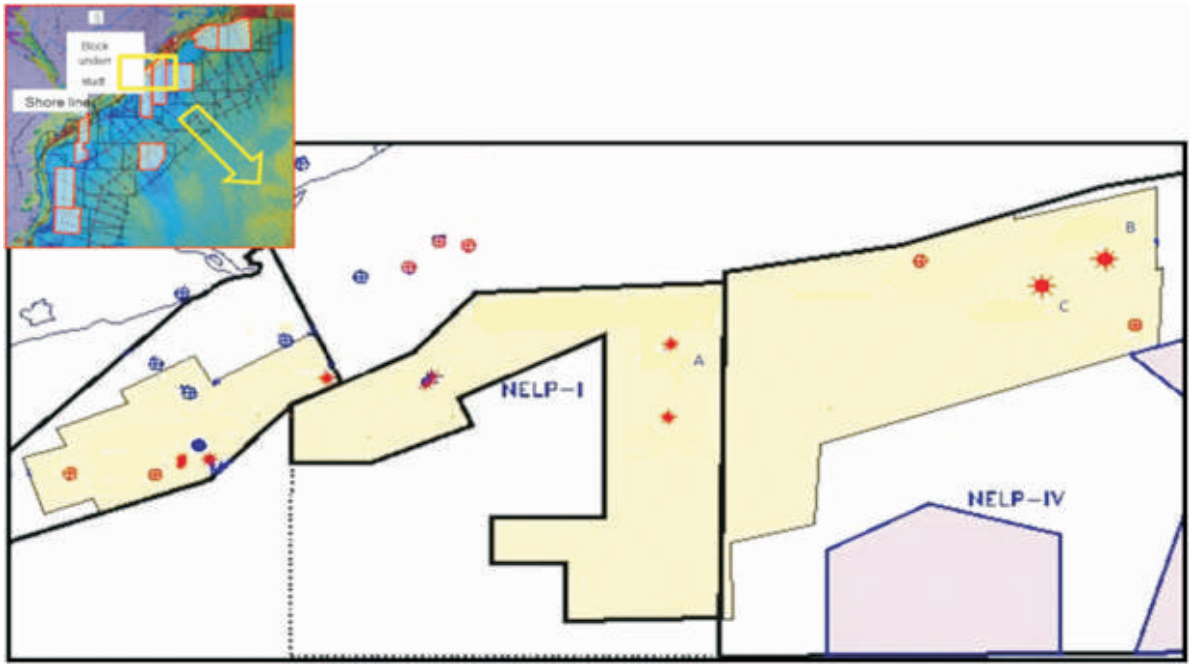

Fig. 2: Location map of the showing three studied wells A, B and C in blocks I and IV.

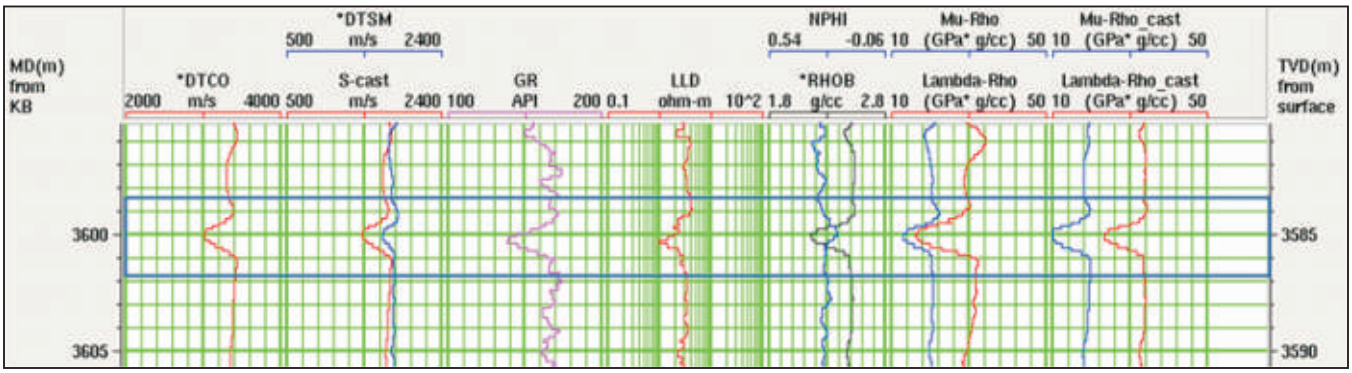

Fig. 3: One meter Gas sand in the interval 3599.5 to 3600.5 (enclosed in gray rectangle)

Table 1: Well logged Vp, Vs and density against marginally charged gas sand have been utilized to calculate Vp, Vs and density for brine sand using Gassmann equation/Castagna transform and density porosity relation;showing brine sand having lower Vs than the shale Vs.

lithology	Vp(m/s)	Vs (m/s)	Density (g/cc)	Remark
Shale	3400 (logged)	1800 (logged)	2.5(logged)	Porosity worked out to be
Gas sand	3000 (logged)	1650 (derived for 80% of gas saturation assuming logged Vs1600m/sis against 30%)	2.07 (derived for 80% of gas saturation assuming logged density 2.18 g/cc against 30%)	0.245 using 2.65, 1 and 0.13g/cc densities for sandstone matrix, water and gas respectively.
Water sand	3250 (derived fromVs for water sand using Castagna transform)	1500 (derived for 100 % of water saturation assuming logged Vs 1600 m/s for 70% Sw)	2.245 (derived for 100% of water saturation assuming logged density 2.18g/cc for 70% Sw)	

Two number of three layered models having sand encompassed in shale have been built from the parameters Vp, Vs and density observed in shale and derived from elastically anomalous sand interval assuming this to be the marginally gas charged sand. First model is built for 80% of gas saturation populating layer with logged Vp, and calculated density and Vsfrom logged Vs and logged density assuming logged sand to be 30% gas saturated. Second model is built for 100% of water saturation populating layer with density and Vs calculated from logged Vs and logged density and Vp calculated from well logged Vs using Castagna transform. Density for 80% gas and 100% water saturated sands is calculated after deriving porosity from the logged density assuming sand of matrix of density 2.65g/cc is 30% charged with gas and rest with water, and Vs for these two cases is worked out from logged Vs with same assumption of saturations. Vp, Vs and density worked out for sands in these two models are given table1.

Frasier decomposition of contribution of amplitude variation with angles to total AVO response intwo cases of low impedance viz gas and brine sands of negative ΔVp, negative Δρ and negative ΔVs (Fig. 4) is discussed hereby.

- Magnitude of ΔVp at brine sand shale interface is smaller than gas sand shale interface, therefore contributing to lesser vegradient thangas sand.
- Magnitude of Δρ at brine sand shale interface is smaller than that of the gas sand shale interface, therefore contributing to lesser +ve gradient than gas sand.
- Magnitude of ΔVs at brine sand shale interface is higher than that of the gas sand, therefore contributing more towards +ve gradient in comparison to than gas sand.
- Combined +ve contribution from ΔVs and Δρ is higher than -ve gradient contributions from ΔVp in boththe brine and gas sand cases; therefore total positive gradient response in Richards and Frasier decomposition. However,
- Comparatively smaller -ve gradient contributions from ΔVp and higher +ve contribution from ΔVs in case of brine sand than the ve gradient contribution from ΔVp and +ve contribution from ΔVs gas sand case, results into total higher positive gradient response from brine sand in comparison to gas sand (Fig.4).
- Therefore, low-impedance brine sands (therefore, lower shear impedance than the interfacing shale) shows lower intercept and higher gradient of decrease in amplitude with offset when compared with class IV gas sand.

Intercept (A) and gradient (B) calculated from Vp, Vs and densities of the layers across the interface using formulae for both the models are cross plotted (Fig.5). Since the AVO gradient from class IV brine sand is almost identical to the gradient from class IV gas sand, these gas sands may be difficult to detect by comparing partial offset stacks or using product (A&B) indicators. However, they do get expressed on A-B cross plot and indicators such as Smith and Gidlow's fluid factor (Gidlow, P. M., Smith, G. C., and Vail, P. J., 1992).

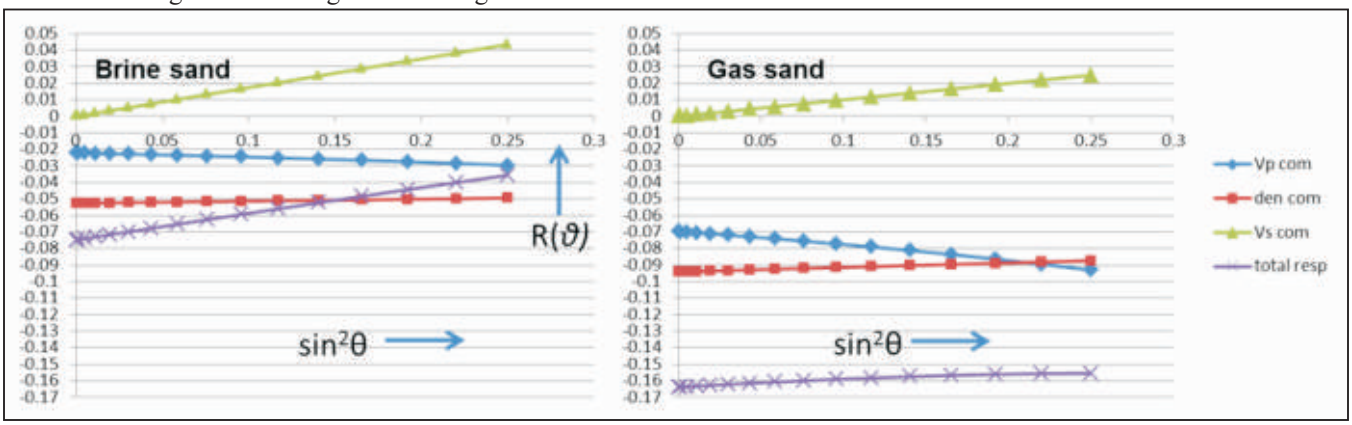

Fig. 4: Frasier decomposition showing contribution coming from change in Vp, Vs and density for brine and gas sands.

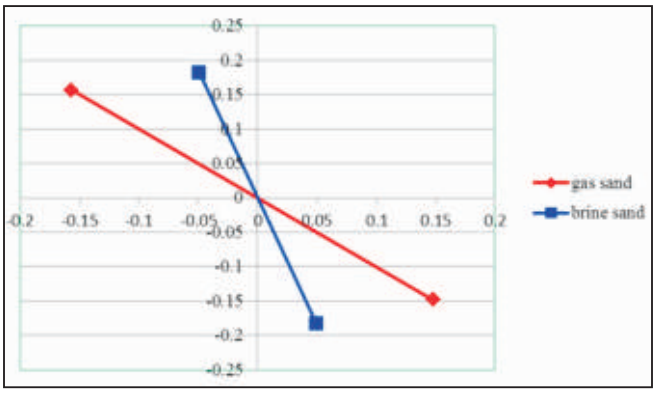

Fig. 5: Gas and brine sands showing two distinct trends on Intercept and Gradients crossplot.Intercept is higher and gradient is smaller corresponding to the sand as compared to the brine sand forming the background trend.

Conclusions

AVO anomaly modeled to be generated by gas sand of 1m thickness encompassed in compacted shale in Mio-Pliocene section in the blocks indicating class IV situations exist in the basin. Sands are deposited in plenty in Mio-Pliocene section and also occasionally gas charged, therefore, thicker class IV gas sands are likely to be encountered besides class III and class II. More deliberate attempt to look for class IV Gas sands along with class III and II may add gas reserves.

Acknowledgements

Authors are thankful to ONGC for permitting to publish the work as the technical paper. Views expressed in the paper are those of the authors only. The paper is part of the project work carried out at ONGC, Kolkata and IRS, ONGC, Ahmedabad. Authors express their gratitude to SV Rao, Ex Director (Expl.),ONGC for assigning the project.Authors are thankful to PP Deo, IRS for technical support through discussions.

References:

Castagna, J.P. and Swan H.W., 1997, Principle of AVO crossplotting: The Leading Edge v.116, no. 4, pp. 337-342.

Castagna, J.P. and Swan H.W., and Foster, D.J., 1998, Framework for AVO gradient and Intercept interpretation: Geophysics, 63, 948-956.

Richards, P.G., and Frasier,C.W., 1976, Scattering of elastic wave fromdepth-dependent in homogeneities: Geophysics, 41, 441458.

Gidlow, P. M., Smith, G.C., and Vail, P.J., 1992, Hydrocarbon detection using fluid factor traces, a case study: How useful isAVO analysis? Joint SEG/EAEG summer research workshop,Technical Program and Abstracts, 78-89.

D.J. Foster, and R.G. Keys, Interpreting AVO Responses SEG 1999, Expanded Abstracts.

D.J. Foster, R.G. Keys, and F. David Lane, 2010, Interpretation of AVO anomalies, Geophysics, 75, 5A375A13. 10.1190/1.3467825.

W.J. Ostrander Plane-wave reflection coefficients for gas sands at nonnormalangles of incidence GEOPHYSICS, VOL. 49, NO. IO (OCTOBER 1984); P. 1637-1648.